Type 1 Interferons Potentiate Human CD8$^+$ T Cell Cytotoxicity Through a STAT4 and Granzyme B Dependent Pathway

Short Running Title: Interferon Induced T cell cytotoxicity

Brittney N. Newby[1], Todd M. Brusko[1], Baiming Zou[2], Mark A. Atkinson[1], Michael Clare-Salzler[1], and Clayton E. Mathews[1]*

[1]-Department of Pathology, Immunology and Laboratory Medicine, University of Florida, Gainesville, FL, USA.

[2]-Department of Biostatistics, College of Public Health and Health Professions & College of Medicine, University of Florida, Gainesville, FL, USA.

***Corresponding Author:**

Clayton E. Mathews, PhD.

Department of Pathology, Immunology and Laboratory Medicine

University of Florida College of Medicine

1275 Center Drive, Biomedical Sciences Building J597

P.O Box 100275, Gainesville, FL 32610.

Email Address: clayton.mathews@pathology.ufl.edu

TEL: (352) 273-9269

ORCID: 0000-0002-8817-6355

Word Count: 4297, Abstract: 144, Figs: 5, Tables: 1, References: 62

Events defining the progression to human type 1 diabetes (T1D) have remained elusive owing to the complex interaction between genetics, the immune system, and the environment. Type 1 Interferons (T1-IFN) are known to be a constituent of the auto-inflammatory milieu within the pancreas of patients with T1D. However, the capacity of IFNα/β to modulate human activated auto-reactive $CD8^+$ T cell (CTL) responses within the islets of patients with T1D have not been investigated. Here, we engineer human beta cell specific CTLs and demonstrate that T1-IFN augments cytotoxicity by inducing rapid phosphorylation of STAT4, resulting in direct binding at the granzyme B (GZMB) promoter within 2 hours of exposure. The current findings provide novel insights concerning the regulation of effector function by T1-IFN in human antigen-experienced $CD8^+$ T cells and provide a mechanism by which the presence of T1-IFN potentiates diabetogenicity within the autoimmune islet.

Essential for the development and implementation of effective therapies for prevention or reversal of type 1 diabetes (T1D) is a detailed understanding of the molecular pathways and cellular interactions that result in beta cell destruction. The hallmark pathological lesion of T1D is a heterogeneous inflammatory cell infiltrate termed insulitis (1; 2). $CD8^+$ T cells, a major component of insulitis, are widely believed to be the primary immune cell responsible for loss of insulin producing beta cells (2; 3). Studies in the NOD mouse model of T1D indicate that $CD8^+$ T cells gain effector activity following islet entry, suggesting signals within the islet microenvironment potentiate lymphocytoxicity (4).

Type 1 interferons (T1-IFN) provide a candidate signal responsible for facilitating beta cell destruction. Case studies describing the induction of autoantibodies and T1D in individuals receiving T1-IFN therapies for chronic hepatitis and cancer have been reported (5). IFNα subtypes have been detected in the islets and circulation of patients with T1D and possess the capacity to enhance expansion and differentiation of cytotoxic T lymphocyte (CTL) (6-13). Beyond this, T1D-associated genes, involved in the induction, signaling, and regulation of the IFNα/β signaling pathway include *IFIH1*, *TYK2*, *STAT4,* and *PTPN2* (14). Although knockout of the IFN-alpha receptor (IFNAR) in NOD mice has produced results to the contrary, a preponderance of evidence in pre-clinical models also supports a pathogenic role for T1-IFN in T1D (15-18). For example, CRISPR-Cas9 deletion of the IFNAR1 subunit in LEW.1WR1 rats delays spontaneous and Poly I:C induced diabetes (17). Additionally, studies revealed that overexpression of IFNα in pancreatic beta cells of non-diabetes-prone mice regulates the onset of diabetes in mice with severe insulitis, while expression of IFNβ in islets of NOD mice accelerated autoimmunity (19-21). However, little is known regarding the mechanisms by which these cytokines direct immune responses within this microenvironment.

T1-IFN constitute an essential component of the innate immune response to viral infection and are known as potent immune-modulators (22). This family of cytokines displays Janus-like activity with ability to activate all seven STAT molecules downstream of IFNAR (23; 24). T1-IFN is a critical signal

for the development of full differentiation and cytotoxicity by mouse CTL, which are dependent upon the balance between STAT1 and STAT4 signaling (6; 25; 26). At present, a robust delineation of the T1-IFN signaling mechanisms in human antigen-experienced CTLs has not been determined.

Over the past decade, the identification of T cell receptors (TCR) specific for tumor antigens has enabled the successful cloning and use of TCR gene transfer for cancer adoptive cell therapies while also advancing the understanding of tumor-infiltrating lymphocyte biology (27). This methodology has been adapted for studies in T1D, where autoantigen-reactive T cell receptors from patients have been identified and cloned, allowing for engineering of primary human $CD8^+$ T cells that express a beta cell-specific αβ TCR (28; 29). One prime example is the identification of a human CTL TCR specific for islet specific glucose 6 phosphatase catalytic subunit (IGRP) that displays beta cell autoreactivity (30-32). For this study, we engineered IGRP specific CTL-avatars to investigate T1-IFN signaling mechanisms that regulate human CTL effector function immediately following T1-IFN exposure. The current findings define a novel mechanism where T1-IFN potently induce cytotoxic function in human CTL through rapid phosphorylation of STAT4, resulting in direct binding of phospho-STAT4 to the granzyme B (GZMB) promoter. These data also provide a mechanistic link between T1-IFN found within the islet microenvironment and regulation of CTL function that favors autoimmune destruction of beta cells.

RESEARCH DESIGN AND METHODS

Study subjects

Peripheral blood mononuclear cell (PBMC) samples were obtained from normal healthy donors through the University of Florida-Diabetes Institute (UFDI) Studybank or from leukopak samples obtained from LifeSouth Community Blood Centers (Demographic information: Table 1). Human islets from human HLA-A*02-01 positive donors were obtained from the Integrated Islet Distribution Program (IIDP). All studies were approved by the University of Florida Institutional Review Board (IRB).

Materials and culture media

T cells and BetaLox5 cells (βL5), an immortalized human β-cell line, were cultured in complete RPMI (cRPMI) and complete DMEM (cDMEM) as previously published (33). Cytokines used for these studies included: IFNα2 and IFNβ1 (Pbl Interferon Source), recombinant human IFNγ (rhIFNγ; R&D), and IL-2 (Preprotech). Information regarding antibodies, TaqMan Probes, and Chip Primer pairs utilized in this study can be found in Supplementary Tables 1-3, respectively. For all studies, cells were cultured at 37°C in an atmosphere containing 5% CO_2

Generation of human antigen specific $CD8^+$ T Cell avatars

$CD8^+$ T cells were negatively selected using RosetteSep™ Human $CD8^+$ T Cell Enrichment Cocktail (Stemcell). Afterwards, naïve $CD8^+$ T cells ($CD8^+CD45RA^+CD45RO^-$) were typically purified to 91.0% $\pm$ 2.5% purity by FACS (Aria III, BD Biosciences). Lentiviral transduction with vectors containing TCR expression constructs pCCL.IGRPopt.eGFP recognizing the autoantigen IGRP (29; 34) or LV.Mart1.TCR.RK recognizing the non beta cell antigen MART1 (27; 35) and subsequent T cell expansion were carried out as outlined in Supplemental Fig. 1. CTL-avatars were cryopreserved after 9 days of expansion.

T1-IFN treatment of CTL

Following removal from liquid nitrogen and equilibration in cDMEM for one-hour, CTL-avatars were treated with IFNα2, IFNβ1, IFNγ, or left untreated for two-hours. After treatment, CTL-avatars were washed twice with PBS (Corning) and were either immediately lysed or re-suspended in complete DMEM for use in cellular assays.

Chromium release assays (CML)

Primary human islets or βL5 cells were used as target cells in the CML assays as previously described (36). Human islets from donors with HLA-A*02 were selected. Prior to plating, human islets were washed with PBS and dispersed in cell dissociation buffer (Life Technologies) for 10 minutes at 37^{o}C with gentle pipetting every 3 min. Dispersed islet cells were plated at 40,000 cells/well. βL5 cells express IGRP in the context of HLA-A*0201 and were seeded at 10,000 cells/well in 96-well flat bottom plates. CML were performed as described previously using IGRP CTL-avatars as effectors (37). Specific lysis was calculated as follows: [(Experimental release – Spontaneous Release)/(Maximum Release – Spontaneous Release)] x 100. For inhibition of granule exocytosis, CTLs were incubated with 100nM of concanamycin A (CMA; Sigma) for 2 hours. For inhibition of Fas Ligand (FasL)-mediated killing or caspase activation, 0.5μg/mL of anti-Fas blocking antibody or 50μM of the pan-caspase inhibitor, Z-VAD-FMK (BD Biosciences), respectively, was added to target cells 2 hours prior to co-culture with CTLs.

Flow cytometry

Subsequent to cytokine treatment, cells were washed and cultured for an additional 4 hours in cytokine free cDMEM containing monensin. Intracellular flow cytometry staining was performed according to standard procedures for the Nuclear Factor Fixation and Permeabilization Buffer set (BioLegend). Live/Dead Near-Infrared dye (Thermo-Fisher) was used to determine viability. Transduction efficiency

was detected by eGFP expression and tetramer staining (Fig. S2). CTLs were analyzed using a LSRFortessa (BD Biosciences) and FlowJo Software (TreeStar).

Western blotting

Western blots were performed as formerly described (38). Proteins were resolved on 4-20% SDS-PAGE gels. Blots were probed with primary antibodies (Supplemental Table 1), bands detected using HRP-linked secondary antibodies, and an ECL detection system (GE Healthcare). Images were captured with an Alpha Innotech FluorChem HD2.

CTL inhibition

Treatment with rapamycin or lisofylline (Cayman Chemical) was performed for 16 hours. Afterwards cells were washed in PBS and treated with IFNα as described. Due the ability of rapamycin to inhibit mTORc1, an important regulator of widespread protein synthesis, we normalized the GZMB protein expression to their respective controls to correct for decreased protein expression observed with rapamycin treatment alone (39).

siRNA knockdown

Accell SMARTpool small interfering RNAs against STAT1, STAT4, GZMB, GAPDH, as well as non-targeting negative control siRNA, and siRNA delivery media were purchased from GE Healthcare Dharmacon. Knockdown in CTL was performed in Accell siRNA delivery media supplemented with IL-2 (100U/mL) according to the manufacturer's protocol. After 72 hours, cells were harvested for gene expression, flow cytometry, and functional assays. Specificity and delivery efficiency of the siRNAs were evaluated using non-targeting control siRNAs.

Gene expression

Total RNA was isolated using the RNeasy Micro Kit (Qiagen) and reverse transcribed using the iScript cDNA Synthesis Kit (BioRad) according to the manufacturer's protocol. TaqMan gene expression primer and probe sets (Supplemental Table 2) were purchased from Applied Biosystems. All gene expression experiments were performed in quadruplicate on a Roche Lightcycler 480 and normalized to 18S.

Chromatin immunoprecipitation

Activated and expanded human CTLs (5 x 10^6) were treated with or without IFNα (1000U/mL) for one hour. Chromatin immunoprecipitation (CHIP) was carried out using the SimpleCHIP Kit (Cell Signaling) per manufacturer's instructions. Chromatin-protein complex immunoprecipitations were performed using 2µg of antibody (Supplementary Table 1). Oligonucleotides specific to the promoter of GZMB were designed using Primer 3 (primer3.ut.ee). Immunoprecipitated DNA was quantified by qPCR using SYBR Green (Qiagen) on the Roche Lightcycler 480. Data are expressed as a percentage of input.

Statistical analysis

All statistical analyses were performed using Prism software (Graphpad). Statistical hypothesis tests were conducted by using non-parametric Wilcoxon sign-rank test. Statistical significance was defined as $P<0.05$.

RESULTS

Acute exposure of CTLs to T1-IFN increases beta cell lysis

While T1-IFN are observed in the islets of deceased donors with T1D, no studies to date have elucidated the impact of these cytokines on infiltrating CTL (8). To model CTL interactions with beta cells *in vitro,* we developed a protocol to generate antigen-specific CTL by lentiviral TCR gene transfer using an IGRP-reactive human TCR (**Fig. S1**; (30; 32; 34)). These functional CTL-avatars recognize $IGRP_{(265\text{-}273)}$ presented in the context of HLA-A*0201 as shown by dextramer staining and display markers characteristic of cytotoxic T effector cells (**Fig. S2-S4**). IGRP-avatars were exposed to IFNα (1000U/mL), IFNβ (500U/mL), or IFNγ (1000U/mL) for 2 hours prior to use in cytotoxicity co-culture assays using primary human islets as targets. IGRP-avatars primed with IFNα (**Fig. 1*A***) or IFNβ (**Fig. 1*B*)** displayed a significantly increased ability to lyse target primary human islets. In contrast, priming with the Type II-IFN (IFNγ) did not enhance cytotoxicity (**Fig. 1*C***). Moreover, this phenotype was maintained over several effector to target (E:T) ratios with IFNα (**Fig. 1*D***) or IFNβ (**Fig. 1*E*)** enhancing the lysis of target βL5 cells at each ratio tested. Similar to the studies with primary islets as targets, priming the IGRP-CTL with IFNγ for 2 hours did not enhance cytotoxicity (**Fig. 1*F***). While significant donor-to-donor variation was observed in the ability of CTL to lyse islet cells (**Figs 1*A*-1*C***) or βL5 cells (**Fig. 1*D*-1*F*, and Supplemental Table 2**), overall the 2 hour exposure of each donor's CTL to IFNα (**Fig. 1*A*, 1*D*, and Supplemental Table 2**) as well as IFNβ (**Figs 1*B*, 1*E*, and Supplemental Table 2**) resulted in an increased capacity to lyse target beta cells.

Patients with recent-onset T1D display increased serum concentrations of T1-IFN when compared to individuals without T1D. This may be indicative of T1-IFN within affected islets, where compartmentalized concentrations of these cytokines may be higher than detected in the sera (40; 41). Thus, we performed a dose titration to investigate whether T1-IFNs could increase CTL activity at concentrations similar to those found in recent onset patients. T1-IFN augmented CTL targeted beta cell

lysis in a dose-dependent manner (**Fig. 1*G***) supporting the notion that exposure of autoreactive T cells to these cytokines enhances function.

Short-Term exposure of CTL to T1-IFN increases cytotoxicity through enhanced GZMB expression

Licensed CTL execute their cytotoxic activities through multiple mechanisms. Specifically, effector CTL produce inflammatory cytokines and mediate targeted killing by expression of death ligands (i.e., FasL), as well as exocytosis of granule components including perforin and granzyme (42). To examine the underlying molecular pathways responsible for T1-IFN induced cytolytic effector function, IGRP-reactive CTL-avatars were treated with T1-IFN for 2 hours and assessed for the expression of IFNγ, FasL, and GZMB by flow cytometry after 4 hours of incubation in media (without antigen stimulation) or in the presence of βL5 cells (antigen stimulated) (**Fig. 2*A*-2*I***). No adverse effects on viability were observed following T1-IFN stimulation (**Fig. S5**). Granzyme B was significantly increased upon T1-IFN priming of the IGRP-CTL-avatars (**Fig. 2*A*-2*C***). No significant changes were observed in the expression of intracellular IFNγ (**Fig. 2*D* and *F***) or surface FasL when compared to the non-primed or IFNγ-primed controls (**Fig. 2*G*-2*I***). Given that we obtained a range of TCR transduction efficiencies with the IGRP-CTL-avatars generated from the 19 donors (median, range 30-95%; **Table 1**), we were able to gate on GFP-reporter positive or negative CTL, the latter serving as an internal control. This allowed us to assess the impact of TCR ligation on effector phenotype. For all three output measures (GZMB, IFNγ, and FasL), the TCR transduced and non-transduced cells were indistinguishable (**Fig. 2**). This observation suggests that T1-IFN conditions CTL to enhance lytic potential through increasing GZMB protein levels in a manner that does not require concomitant ligation with cognate antigen and signaling through the TCR.

Next, inhibitors were employed to block T1-IFN induced IGRP-CTL cytotoxicity during CML assays (**Fig. 2*J*-*M***). These included a neutralizing antibody to the Fas receptor on beta cells to block Fas-FasL interactions; Concanamycin A, a V-ATPase inhibitor to prevent the release of cytotoxic

granules from CTL; and Z-VAD-FMK, a pan-caspase inhibitor to counteract activation of caspases and granzymes within beta cells. Fig.Inhibition of Fas-FasL interactions did not abrogate the T1-IFN-induced gain in IGRP-avatar cytotoxicity (**Fig. 2*K***). However, prevention of granule exocytosis and release of GZMB by CTL-avatars using Concanamycin A abolished the increased cytotoxicity seen in T1-IFN primed IGRP-CTL-avatars (**Fig. 2*L***). Similarly, Z-VAD-FMK inhibition of protease activity (caspases and granzymes) in βL5 cells resulted in protection from IGRP-CTL-avatar-mediated destruction (**Fig. 2*M***).

Rapid T1-IFN signaling is STAT-dependent and requires neither T-bet, Eomes, nor mTOR

T1-IFN employ several non-canonical signaling pathways to induce their pleiotropic effects and have the ability to activate all members of the STAT family (24). STAT1 and STAT4 are heavily linked to effector T cell function in murine models (43; 44). Therefore, we hypothesized that STAT1 and STAT4 regulate T1-IFN responses in activated IGRP-CTL-avatars. Thus, CTL-avatars were treated with IFNγ (1000U/mL) or several concentrations of IFNα or β for 15 minutes. Phosphorylated and total STAT1 and STAT4 were assessed by western blot. T1-IFN induced a robust dose dependent phosphorylation of both STAT1 and STAT4, while the total levels of STAT1 and STAT4 among the groups remained equal (**Fig. 3*A-C***). Next, we performed time-course analysis and observed that the phosphorylation of STAT1 peaks 30 minutes following T1-IFN exposure, while STAT4 phosphorylation remains highly elevated over the 2-hour time course (**Fig. 3*D-F***). We were able to confirm these results by phospho-flow cytometry, whereby activation of STAT1 was rapid, peaking between 15 and 30 minutes and returning to baseline by 2 hours (**Fig. 3*G* and *H***). STAT4 reached maximal activation by 30 minutes and remained elevated out to 2 hours (**Fig. 3*G* and *I***). IFNα was unable to induce phosphorylation of STAT5 and STAT6 but did display minimal activation of STAT3 (**Fig. S6**) suggesting that STAT1 and STAT4 are the preferential T1-IFN signaling mediators in during acute IFNα exposure in activated IGRP-CTL-avatars.

Previous studies performed in mouse models demonstrate that T1-IFN regulate transcriptional programs induced by T-bet and Eomes, which are known to be essential for differentiation and development of human CTL effector function (25; 45). Additionally, these transcription factors were up-regulated in mouse CTL exposed to IFNα and reported to specifically bind the promoters of IFNγ, perforin, and GZMB (46). Since T1-IFN rapidly act to increase effector function through the upregulation of GZMB in activated antigen-specific T cells, we reasoned that these cytokines could be indirectly inducing this phenotype through T-bet or Eomes. Therefore, we examined expression of T-bet and Eomes in IGRP-CTL-avatars following a 2-hour T1-IFN exposure followed by 4 hours of incubation in media (without antigen stimulation) or in the presence of βL5 cells (antigen stimulated). Intriguingly, neither T-bet nor Eomes displayed increased expression after short-term incubation with IFNα or IFNβ (**Fig. 3*J* and *K***) alone or in the presence of βL5 cells (antigen stimulated), suggesting that these transcription factors are not involved in the regulating GZMB following short-term T1-IFN treatment.

T1-IFN have also been reported to regulate translation of interferon stimulated genes through the activation of mTOR kinase activity (47). mTOR integrates environmental cues to direct cellular metabolism and plays a role in T cell activation and differentiation (48). We assessed the impact of rapamycin-mediated mTOR inhibition on the rapid upregulation of GZMB detected after short-term T1-IFN treatment. Two concentrations of rapamycin were chosen to correlate with inhibition of mTOR complex 1 (at the lower concentration of 1nM) and inhibition of both mTORc1 and mTORc2 (at higher concentrations of 1μM) (49). IGRP-CTL-avatars were pre-treated for 16 hours with rapamycin, primed with IFNα for 2 hours, and assessed by flow cytometry. Rapamycin had no effect on CTL-avatar viability (data not shown) or the T1-IFN-mediated increase in GZMB expression (**Fig. 3*L***). These data suggest that regulation of GZMB by T1-IFN in $CD8^+$ T cells is independent of TORC1 and TORC2 complexes.

Enhanced GZMB expression induced by T1-IFN priming of activated CTLs is dependent upon STAT4-activation.

To investigate the whether the signaling mediators STAT1 and STAT4 are necessary for the T1-IFN induction of GZMB and heightened lysis of target cells, we employed small interfering RNAs (siRNAs) to reduce the levels of STAT1 or STAT4. CTL were transfected with STAT1 or STAT4-specific siRNAs for 72 hours. qRT-PCR confirmed efficient and specific mRNA knockdown of STAT1 and STAT4 mRNA by their corresponding siRNAs (**Fig. 4*A* and *B***). Next, siRNA transfected IGRP-CTL-avatars were primed with T1-IFN and assessed for GZMB production. Non-targeting control transfected CTL displayed an increase in GZMB after priming with IFNα (1000U/mL; **Fig. 4*C* and *D***). Transfection of IGRP-avatars with siRNAs had no adverse effect on viability (**Fig. 4*E***). CTL-avatars transfected with STAT1-specific siRNA displayed similar levels of T1-IFN induced GZMB when compared to controls, while in CTL-avatars where STAT4 was reduced by siRNA displayed a significant loss in T1-IFN induced GZMB (**Fig. 4*C* and *E***). These data confirm that STAT4 is critical for T1-IFN induced amplification of CTL-avatar effector function through GZMB production.

Lisofylline is an anti-inflammatory agent known to prevent IL-12 induced activation of STAT4 and has been used in combination with other therapeutics for the reversal of autoimmune diabetes in the NOD mouse (50; 51). To confirm that STAT4 is critical for the early and rapid induction of Granzyme B by T1-IFN, we asked whether lisofylline could prevent T1-IFN induced STAT4 activation in our model. IGRP-CTL-avatars were pre-treated for 16 hours with lisofylline. Lisofylline exhibited no adverse effect on viability (data not shown). The ability of lisofylline to inhibit phosphorylation of STAT4 was confirmed by immunoblot and phosphoflow analysis (**Fig. 4*F* and *G***). Lisofylline also prevented T1-IFN-mediated induction of GZMB (**Fig. 4*H* and *I***). These data confirm the importance of STAT4 for GZMB production in response to T1-IFN and also suggest that lisofylline can act to reduce auto-inflammation by modulating CTL responses to T1-IFN.

Activation of pSTAT4-Tyr693 by T1-IFN leads to increased transcription of GZMB through direct promoter binding

Previous studies conducted in primary human T cells showed that IFNα-induced tyrosine phosphorylation of STAT4 (pTyr693) and this activation led to DNA binding (52). We hypothesized that the rapid accumulation of CTL-avatar effector function observed after short-term T1-IFN priming was due to binding of pSTAT4 to the *GZMB* promoter and transcriptional activation. To investigate this hypothesis, we first performed qRT-PCR to verify that GZMB transcript levels were increased upon short-term priming by T1-IFN. Indeed, T1-IFN significantly increased GZMB expression (**Fig. 5*A***). IGRP-CTL-avatars also display a robust T1-IFN response with the induction of *IFIH1*, a well-known interferon-stimulated gene (**Fig. 5*B***). Utilizing the JASPAR database (53), we interrogated the *GZMB* promoter for putative binding sites for STAT1 and STAT4, which yielded one binding site 67-80 base pairs upstream of the *GZMB* transcription start site (TSS) and two additional distal binding sites within a region 625-650bp upstream of the TSS. Oligonucleotides were designed to amplify regions of DNA that were in close proximity of these binding sites (schematics found in **Fig. S7**). There was no observed binding of pSTAT1 or total STAT1 to the *GZMB* promoter following IFNα priming at either the proximal or distal site. This confirmed that STAT1, in this context, is not required for regulation of GZMB following acute T1-IFN exposure. Priming of activated CTL-avatars with IFNα resulted in increased binding of pSTAT4-Tyr 693 but not tSTAT4 to the *GZMB* promoter. pSTAT4 binding was only observed at the proximal binding site located 67-80bp upstream of the *GZMB* TSS (**Fig. 5*C***). Thus T1-IFN rapidly induces pSTAT4 that directly binds to the *GZMB* promoter (**Fig. 5*C***) to increase transcription (**Fig. 5*A***) and GZMB protein levels (**Fig. 2**), resulting in enhanced CTL cytolytic function (**Fig. 1**).

DISCUSSION

Here, we employ the use of activated antigen-specific human CTL to demonstrate that T1-IFN can induce a remarkably rapid acquisition of effector function through activation and direct binding of pSTAT4 to the *GZMB* promoter. Our data extend previous studies in murine and human T cells demonstrating that T1-IFN can act as a "third signal" cytokine (6; 7; 25). In contrast to previous reports, we have utilized our model to define rapid T1-IFN signaling mechanisms after only 2 hours of exposure, indicating that GZMB is a first responder, rapidly produced to arm antigen-experienced CTL with an increased capacity to kill target cells. Unlike other reports, we did not detect any differences in production of IFNγ or FasL (6; 7; 25). It is likely that the kinetics for the generation of these effector molecules differs from GZMB and may occur by other T1-IFN-induced signaling pathways. Additionally, the diverse activation of downstream signaling pathways by T1-IFN may provoke a feed-forward amplification of this signal (54).

T1-IFN regulate a complex network of signaling pathways, and in order to activate alternative T1-IFN mediated signaling, there must be a disruption in the balance of classically activated STAT1 versus other STAT molecules (23; 24). T1-IFN mediated CTL responses in murine and human cells have been linked to STAT1 and STAT4 signaling downstream of the IFNA-receptor (6; 25; 52). Phosphorylation of STAT4 can be induced through activation of TCR signaling and is reported to counteract the anti-proliferative STAT1 response (43; 44). This is the first study to our knowledge to characterize the kinetics of T1-IFN mediated activation of pSTAT1 versus pSTAT4 in human antigen-experienced CTL. By design, our *in vitro* experiments involve a controlled microenvironment, which limits our ability to definitively deduce signal transduction and cellular responses to the complex cytokine milieu within the pancreatic islet during T1D pathogenesis. In line with mouse models of viral infection, we show that activated human CTL-avatars responding to T1-IFN favor STAT4-dependent signaling over the canonical STAT1-dependent signaling pathway (43). Therefore these pathways likely

function in a positive manner by enhancing clearance of viral infections, but conversely in autoimmune prone individuals arm and enhance pathogenicity of beta cell reactive CTL.

Our results also mechanistically demonstrate that T1-IFN-induced signaling and activation of pSTAT4-Tyr693 leads to direct binding at the proximal promoter of GZMB. Previous studies investigating the transcriptional regulation of GZMB revealed that T cell activation induces mRNA expression, which was mapped to a 243bp promoter element upstream of the GZMB-TSS (55; 56). Mutational analysis and electrophoretic mobility shift assay studies confirmed the binding sites for several transcription factors involved in the activation and differentiation of T lymphocytes including AP-1, Runx1, Ikaros, and CREB1 (57; 58). Apart from these studies, very little is known regarding the transcriptional regulation of GZMB. T1-IFN regulation of GZMB has been largely appreciated through studies carried out in murine and human T cells (6; 7). However, the precise mechanisms and signal transduction pathways required for such induction are largely uncharacterized, typically noted as a consequence of widespread JAK/STAT signaling. In this investigation, our data provides further insight into this regulation. Survey of the GZMB promoter using the JASPAR database led to the identification several overlapping putative binding sites for STAT1 and STAT4. This was not surprising due to the fact that STAT molecules recognize palindromic core sequences with varied binding specificity attributed to nucleotide preference flanking this conserved region (59). It should be noted that the pSTAT4 promoter element -80/-67 bases upstream of the TSS, identified here, is within the T cell-inducible region identified by previous studies. Chromatin remodeling by T1-IFNs is crucial for the rapid induction of interferon-stimulated genes, which could explain the rapid changes occurring at the *GZMB* promoter (25; 55).

Mounting evidence suggests that stimuli within the islet microenvironment contribute to CTL cytotoxicity and precipitate T1D. Studies in the NOD demonstrate that IGRP-reactive NY8.3 $CD8^+$ T cells are initially activated in the pancreatic lymph node but only acquire full cytotoxic capacity when in the islet. This occurs independently of antigen presentation by beta cells (4). Over the years,

investigators have hypothesized that pro-inflammatory cytokines contribute to disease with many efforts focused on elucidating contributions of TNFα, IL-1β, and IFNγ in the NOD mouse model. However, the only cytokine that displays a consistent increase in patients with T1D is IFNα (8; 9). Our *in vitro* model has provided a potential mechanism as to how $CD8^+$ T cells develop enhanced effector function when exposed to T1-IFN. Similar to NY8.3 CTLs found in the NOD islet, this increase in GZMB is global and independent of synergistic antigen-stimulation by the intended target cell. T1-IFN embodies an essential component of the innate immune response to viral infection, a well-known putative environmental factor that has long been associated with the islets of patients with T1D. Furthermore, T1D-risk variants found in *IFIH1*, *TYK2*, and *STAT4* are associated with constitutive activity, augmented T1-IFN signaling, and increased T1-IFN sensitivity, respectively (60-62). Taken together with our current findings, it is likely that a genetic pre-disposition skewed toward dysfunctional T1-IFN responses create an islet environment permissive to enhanced human beta cell-specific cytotoxicity. While the pleiotropic actions of T1-IFN are designed to strengthen the immune response to viral pathogens, this response proves detrimental in the case of autoimmunity where the immune response is misdirected toward self and in this way, can promote beta cell death in T1D.

Author Contributions

B.N.N. conducted experiments. B.N.N, T.M.B, M.C.S., and C.E.M designed experiments. Data analysis, interpretation, and discussion were completed by B.N.N, T.M.B, B.Z., M.A.A, M.C.S., and C.E.M. Manuscript was written and revised by B.N.N, T.M.B, M.A.A, M.C.S., and C.E.M. Study was conceived by B.N.N. and C.E.M. Clayton E. Mathews is the guarantor of this work and, as such, had full access to all of the data contained within this study and takes responsibility for the integrity of the data as well as the accuracy of the data analysis.

Acknowledgements

We would like to thank all of the study participants, as well as Amanda Posgai (University of Florida) and Robert L Whitener (Stanford University) for critical review of the manuscript.

Funding

The current study was partially supported by grants from the National Institutes of Health NIDDK (UC4DK104194, R01DK074656) and NIAID (P01-A1042288). B.N.N was also supported by an NRSA individual fellowship from the NIDDK (F30-DK105788).

Competing Interests

The authors declare that no conflict of interests exist pertaining to the contents of this manuscript.

References

1. Willcox A, Richardson SJ, Bone AJ, Foulis AK, Morgan NG: Analysis of islet inflammation in human type 1 diabetes. Clin Exp Immunol 2009;155:173-181
2. Betts MR, Brenchley JM, Price DA, De Rosa SC, Douek DC, Roederer M, Koup RA: Sensitive and viable identification of antigen-specific CD8+ T cells by a flow cytometric assay for degranulation. J Immunol Methods 2003;281:65-78
3. Serreze DV, Leiter EH, Christianson GJ, Greiner D, Roopenian DC: Major histocompatibility complex class I-deficient NOD-B2mnull mice are diabetes and insulitis resistant. Diabetes 1994;43:505-509
4. Graham KL, Krishnamurthy B, Fynch S, Mollah ZU, Slattery R, Santamaria P, Kay TW, Thomas HE: Autoreactive cytotoxic T lymphocytes acquire higher expression of cytotoxic effector markers in the islets of NOD mice after priming in pancreatic lymph nodes. Am J Pathol 2011;178:2716-2725
5. Nakamura K, Kawasaki E, Imagawa A, Awata T, Ikegami H, Uchigata Y, Kobayashi T, Shimada A, Nakanishi K, Makino H, Maruyama T, Hanafusa T: Type 1 diabetes and interferon therapy: a nationwide survey in Japan. Diabetes Care 2011;34:2084-2089
6. Curtsinger JM, Valenzuela JO, Agarwal P, Lins D, Mescher MF: Type I IFNs provide a third signal to CD8 T cells to stimulate clonal expansion and differentiation. J Immunol 2005;174:4465-4469
7. Hervas-Stubbs S, Riezu-Boj JI, Gonzalez I, Mancheno U, Dubrot J, Azpilicueta A, Gabari I, Palazon A, Aranguren A, Ruiz J, Prieto J, Larrea E, Melero I: Effects of IFN-alpha as a signal-3 cytokine on human naive and antigen-experienced CD8(+) T cells. Eur J Immunol 2010;40:3389-3402
8. Foulis AK, Farquharson MA, Meager A: Immunoreactive alpha-interferon in insulin-secreting beta cells in type 1 diabetes mellitus. Lancet 1987;2:1423-1427
9. Huang X, Yuang J, Goddard A, Foulis A, James RF, Lernmark A, Pujol-Borrell R, Rabinovitch A, Somoza N, Stewart TA: Interferon expression in the pancreases of patients with type I diabetes. Diabetes 1995;44:658-664
10. Lundberg M, Krogvold L, Kuric E, Dahl-Jorgensen K, Skog O: Expression of Interferon-Stimulated Genes in Insulitic Pancreatic Islets of Patients Recently Diagnosed With Type 1 Diabetes. Diabetes 2016;65:3104-3110
11. Lindenmann J, Burke DC, Isaacs A: Studies on the production, mode of action and properties of interferon. Br J Exp Pathol 1957;38:551-562
12. Chehadeh W, Weill J, Vantyghem MC, Alm G, Lefebvre J, Wattre P, Hober D: Increased level of interferon-alpha in blood of patients with insulin-dependent diabetes mellitus: relationship with coxsackievirus B infection. J Infect Dis 2000;181:1929-1939
13. Allen JS, Pang K, Skowera A, Ellis R, Rackham C, Lozanoska-Ochser B, Tree T, Leslie RD, Tremble JM, Dayan CM, Peakman M: Plasmacytoid dendritic cells are proportionally expanded at diagnosis of type 1 diabetes and enhance islet autoantigen presentation to T-cells through immune complex capture. Diabetes 2009;58:138-145
14. Concannon P, Rich SS, Nepom GT: Genetics of type 1A diabetes. N Engl J Med 2009;360:1646-1654
15. Li Q, Xu B, Michie SA, Rubins KH, Schreriber RD, McDevitt HO: Interferon-alpha initiates type 1 diabetes in nonobese diabetic mice. Proc Natl Acad Sci U S A 2008;105:12439-12444
16. Quah HS, Miranda-Hernandez S, Khoo A, Harding A, Fynch S, Elkerbout L, Brodnicki TC, Baxter AG, Kay TW, Thomas HE, Graham KL: Deficiency in type I interferon signaling prevents the early interferon-induced gene signature in pancreatic islets but not type 1 diabetes in NOD mice. Diabetes 2014;63:1032-1040
17. Qaisar N, Lin S, Ryan G, Yang C, Oikemus SR, Brodsky MH, Bortell R, Mordes JP, Wang JP: A Critical Role for the Type I Interferon Receptor in Virus-Induced Autoimmune Diabetes in Rats. Diabetes 2017;66:145-157

18. Lincez PJ, Shanina I, Horwitz MS: Reduced expression of the MDA5 Gene IFIH1 prevents autoimmune diabetes. Diabetes 2015;64:2184-2193
19. Pelegrin M, Devedjian JC, Costa C, Visa J, Solanes G, Pujol A, Asins G, Valera A, Bosch F: Evidence from transgenic mice that interferon-beta may be involved in the onset of diabetes mellitus. J Biol Chem 1998;273:12332-12340
20. Stewart TA, Hultgren B, Huang X, Pitts-Meek S, Hully J, MacLachlan NJ: Induction of type I diabetes by interferon-alpha in transgenic mice. Science 1993;260:1942-1946
21. Carrero JA, Calderon B, Towfic F, Artyomov MN, Unanue ER: Defining the transcriptional and cellular landscape of type 1 diabetes in the NOD mouse. PLoS One 2013;8:e59701
22. Gonzalez-Navajas JM, Lee J, David M, Raz E: Immunomodulatory functions of type I interferons. Nat Rev Immunol 2012;12:125-135
23. Kallal LE, Biron CA: Changing partners at the dance: Variations in STAT concentrations for shaping cytokine function and immune responses to viral infections. Jakstat 2013;2:e23504
24. Platanias LC: Mechanisms of type-I- and type-II-interferon-mediated signalling. Nat Rev Immunol 2005;5:375-386
25. Agarwal P, Raghavan A, Nandiwada SL, Curtsinger JM, Bohjanen PR, Mueller DL, Mescher MF: Gene regulation and chromatin remodeling by IL-12 and type I IFN in programming for CD8 T cell effector function and memory. J Immunol 2009;183:1695-1704
26. Xiao Z, Casey KA, Jameson SC, Curtsinger JM, Mescher MF: Programming for CD8 T cell memory development requires IL-12 or type I IFN. J Immunol 2009;182:2786-2794
27. Morgan RA, Dudley ME, Wunderlich JR, Hughes MS, Yang JC, Sherry RM, Royal RE, Topalian SL, Kammula US, Restifo NP, Zheng Z, Nahvi A, de Vries CR, Rogers-Freezer LJ, Mavroukakis SA, Rosenberg SA: Cancer regression in patients after transfer of genetically engineered lymphocytes. Science 2006;314:126-129
28. Babon JA, DeNicola ME, Blodgett DM, Crevecoeur I, Buttrick TS, Maehr R, Bottino R, Naji A, Kaddis J, Elyaman W, James EA, Haliyur R, Brissova M, Overbergh L, Mathieu C, Delong T, Haskins K, Pugliese A, Campbell-Thompson M, Mathews C, Atkinson MA, Powers AC, Harlan DM, Kent SC: Analysis of self-antigen specificity of islet-infiltrating T cells from human donors with type 1 diabetes. Nat Med 2016;22:1482-1487
29. Driver JP, Racine JJ, Ye C, Lamont DJ, Newby BN, Leeth CM, Chapman HD, Brusko TM, Chen YG, Mathews CE, Serreze DV: Interferon-γ Limits Diabetogenic CD8(+) T-Cell Effector Responses in Type 1 Diabetes. Diabetes 2017;66:710-721
30. Unger WW, Pinkse GG, Mulder-van der Kracht S, van der Slik AR, Kester MG, Ossendorp F, Drijfhout JW, Serreze DV, Roep BO: Human clonal CD8 autoreactivity to an IGRP islet epitope shared between mice and men. Ann N Y Acad Sci 2007;1103:192-195
31. Jarchum I, Nichol L, Trucco M, Santamaria P, DiLorenzo TP: Identification of novel IGRP epitopes targeted in type 1 diabetes patients. Clin Immunol 2008;127:359-365
32. Babad J, Mukherjee G, Follenzi A, Ali R, Roep BO, Shultz LD, Santamaria P, Yang OO, Goldstein H, Greiner DL, DiLorenzo TP: Generation of beta cell-specific human cytotoxic T cells by lentiviral transduction and their survival in immunodeficient human leucocyte antigen-transgenic mice. Clin Exp Immunol 2015;179:398-413
33. Lightfoot YL, Chen J, Mathews CE: Role of the mitochondria in immune-mediated apoptotic death of the human pancreatic beta cell line betaLox5. In *PLoS One* United States, 2011, p. e20617
34. Brusko TM, Koya RC, Zhu S, Lee MR, Putnam AL, McClymont SA, Nishimura MI, Han S, Chang LJ, Atkinson MA, Ribas A, Bluestone JA: Human antigen-specific regulatory T cells generated by T cell receptor gene transfer. PLoS One 2010;5:e11726
35. Johnson LA, Morgan RA, Dudley ME, Cassard L, Yang JC, Hughes MS, Kammula US, Royal RE, Sherry RM, Wunderlich JR, Lee CC, Restifo NP, Schwarz SL, Cogdill AP, Bishop RJ, Kim H, Brewer CC, Rudy SF, VanWaes C, Davis JL, Mathur A, Ripley RT, Nathan DA, Laurencot CM, Rosenberg SA:

Gene therapy with human and mouse T-cell receptors mediates cancer regression and targets normal tissues expressing cognate antigen. In *Blood* United States, 2009, p. 535-546
36. Takaki T, Marron MP, Mathews CE, Guttmann ST, Bottino R, Trucco M, DiLorenzo TP, Serreze DV: HLA-A*0201-restricted T cells from humanized NOD mice recognize autoantigens of potential clinical relevance to type 1 diabetes. J Immunol 2006;176:3257-3265
37. Chen J, Grieshaber S, Mathews CE: Methods to assess beta cell death mediated by cytotoxic T lymphocytes. J Vis Exp 2011;
38. Gusdon AM, Fernandez-Bueno GA, Wohlgemuth S, Fernandez J, Chen J, Mathews CE: Respiration and substrate transport rates as well as reactive oxygen species production distinguish mitochondria from brain and liver. BMC Biochem 2015;16:22
39. Laplante M, Sabatini DM: mTOR signaling in growth control and disease. Cell 2012;149:274-293
40. Chehadeh W, Weill J, Vantyghem MC, Alm G, Lefèbvre J, Wattré P, Hober D: Increased level of interferon-alpha in blood of patients with insulin-dependent diabetes mellitus: relationship with coxsackievirus B infection. J Infect Dis 2000;181:1929-1939
41. Xia CQ, Peng R, Chernatynskaya AV, Yuan L, Carter C, Valentine J, Sobel E, Atkinson MA, Clare-Salzler MJ: Increased IFN-alpha-producing plasmacytoid dendritic cells (pDCs) in human Th1-mediated type 1 diabetes: pDCs augment Th1 responses through IFN-alpha production. J Immunol 2014;193:1024-1034
42. Chavez-Galan L, Arenas-Del Angel MC, Zenteno E, Chavez R, Lascurain R: Cell death mechanisms induced by cytotoxic lymphocytes. Cell Mol Immunol 2009;6:15-25
43. Gil MP, Ploquin MJ, Watford WT, Lee SH, Kim K, Wang X, Kanno Y, O'Shea JJ, Biron CA: Regulating type 1 IFN effects in CD8 T cells during viral infections: changing STAT4 and STAT1 expression for function. Blood 2012;120:3718-3728
44. Nguyen KB, Watford WT, Salomon R, Hofmann SR, Pien GC, Morinobu A, Gadina M, O'Shea JJ, Biron CA: Critical role for STAT4 activation by type 1 interferons in the interferon-gamma response to viral infection. Science 2002;297:2063-2066
45. Kaech SM, Cui W: Transcriptional control of effector and memory CD8+ T cell differentiation. Nat Rev Immunol 2012;12:749-761
46. Glimcher LH, Townsend MJ, Sullivan BM, Lord GM: Recent developments in the transcriptional regulation of cytolytic effector cells. Nat Rev Immunol 2004;4:900-911
47. Kaur S, Lal L, Sassano A, Majchrzak-Kita B, Srikanth M, Baker DP, Petroulakis E, Hay N, Sonenberg N, Fish EN, Platanias LC: Regulatory effects of mammalian target of rapamycin-activated pathways in type I and II interferon signaling. J Biol Chem 2007;282:1757-1768
48. Pollizzi KN, Powell JD: Regulation of T cells by mTOR: the known knowns and the known unknowns. Trends Immunol 2015;36:13-20
49. Sarbassov DD, Ali SM, Sengupta S, Sheen JH, Hsu PP, Bagley AF, Markhard AL, Sabatini DM: Prolonged rapamycin treatment inhibits mTORC2 assembly and Akt/PKB. Mol Cell 2006;22:159-168
50. Yang Z, Chen M, Fialkow LB, Ellett JD, Wu R, Nadler JL: Inhibition of STAT4 activation by lisofylline is associated with the protection of autoimmune diabetes. Ann N Y Acad Sci 2003;1005:409-411
51. Yang Z, Chen M, Carter JD, Nunemaker CS, Garmey JC, Kimble SD, Nadler JL: Combined treatment with lisofylline and exendin-4 reverses autoimmune diabetes. Biochem Biophys Res Commun 2006;344:1017-1022
52. Cho SS, Bacon CM, Sudarshan C, Rees RC, Finbloom D, Pine R, O'Shea JJ: Activation of STAT4 by IL-12 and IFN-alpha: evidence for the involvement of ligand-induced tyrosine and serine phosphorylation. J Immunol 1996;157:4781-4789
53. Mathelier A, Fornes O, Arenillas DJ, Chen CY, Denay G, Lee J, Shi W, Shyr C, Tan G, Worsley-Hunt R, Zhang AW, Parcy F, Lenhard B, Sandelin A, Wasserman WW: JASPAR 2016: a major

expansion and update of the open-access database of transcription factor binding profiles. Nucleic Acids Res 2016;44:D110-115
54. Ivashkiv LB, Donlin LT: Regulation of type I interferon responses. Nat Rev Immunol 2014;14:36-49
55. Hanson RD, Ley TJ: Transcriptional activation of the human cytotoxic serine protease gene CSP-B in T lymphocytes. Mol Cell Biol 1990;10:5655-5662
56. Haddad P, Wargnier A, Bourge JF, Sasportes M, Paul P: A promoter element of the human serine esterase granzyme B gene controls specific transcription in activated T cells. Eur J Immunol 1993;23:625-629
57. Hanson RD, Grisolano JL, Ley TJ: Consensus AP-1 and CRE motifs upstream from the human cytotoxic serine protease B (CSP-B/CGL-1) gene synergize to activate transcription. Blood 1993;82:2749-2757
58. Wargnier A, Legros-Maida S, Bosselut R, Bourge JF, Lafaurie C, Ghysdael CJ, Sasportes M, Paul P: Identification of human granzyme B promoter regulatory elements interacting with activated T-cell-specific proteins: implication of Ikaros and CBF binding sites in promoter activation. Proc Natl Acad Sci U S A 1995;92:6930-6934
59. Yamamoto K, Miura O, Hirosawa S, Miyasaka N: Binding sequence of STAT4: STAT4 complex recognizes the IFN-gamma activation site (GAS)-like sequence (T/A)TTCC(C/G)GGAA(T/A). Biochem Biophys Res Commun 1997;233:126-132
60. Funabiki M, Kato H, Miyachi Y, Toki H, Motegi H, Inoue M, Minowa O, Yoshida A, Deguchi K, Sato H, Ito S, Shiroishi T, Takeyasu K, Noda T, Fujita T: Autoimmune disorders associated with gain of function of the intracellular sensor MDA5. Immunity 2014;40:199-212
61. Marroqui L, Dos Santos RS, Floyel T, Grieco FA, Santin I, Op de Beeck A, Marselli L, Marchetti P, Pociot F, Eizirik DL: TYK2, a Candidate Gene for Type 1 Diabetes, Modulates Apoptosis and the Innate Immune Response in Human Pancreatic beta cells. Diabetes 2015;64:3808-3817
62. Kariuki SN, Kirou KA, MacDermott EJ, Barillas-Arias L, Crow MK, Niewold TB: Cutting edge: autoimmune disease risk variant of STAT4 confers increased sensitivity to IFN-alpha in lupus patients in vivo. J Immunol 2009;182:34-38

Fig. Legends

Fig. 1: Short-term exposure of autoreactive CTL to Type 1 Interferons enhances cytotoxicity toward beta cells. IGRP-specific CTL-avatars (IGRP-CTL) were exposed to interferon α, β, or γ for 2 hours. Cytokines were removed by washing and then IGRP-CTL were co-cultured with dispersed primary human islets (**A-C**) or BetaLox5 cells (βL5) (**D-F**) for 16 hours in a standard chromium release assay (CML). **(A-C)** Box and whisker plots represent the percentage of dispersed human islets lysed by IGRP-CTLs. Data for the interferon-mediated change in effector function for each individual T cell donor is provided using a scatter plot with connecting lines. **(D-F)** Lines represent the percentage of specific lysis induced by IGRP-CTL primed with IFNα (1000U/mL: **A and D**), IFNβ (500U/mL: **B and E**), or IFNγ (1000U/mL: **C and F**) over several effector to target ratios (E:T). **(G)** IGRP-CTL were primed with various concentrations of T1-IFN for 2 hours and co-cultured with βL5 at a 10:1 E:T for 16 hours in CML assays. Data are plotted as mean ± SEM where T cells from each donor (7 donors for **A-C**, 6 donors for **D-F**, and 5 donors for **G**) were weighted equally. There were at least three separate experiments for each donor. Statistical significance was assessed using a non-parametric paired T-test with Wilcoxon Post Test Analysis. * $P<0.05$; ** $P<0.01$; *** $P<0.001$

Fig. 2: Granzyme B Expression is increased upon T1-IFN priming of Autoreactive CTLs.

(A-I) IGRP-CTL were primed with IFNα, IFNβ, or IFNγ for 2 hours. Cytokines were removed by washing and then IGRP-CTL were incubated for an additional 4 hours in media or stimulated by co-culture with βL5 cells. Representative histograms and mean fluorescence intensities for (**A-C**) GZMB, (**D-F**) IFNγ, and (**G-I**) Fas Ligand are displayed. **(J-M)** To the determine the contribution of pathways important for CTL-mediated killing, IGRP-CTL were co-cultured with βL5 cells (10:1 – E:T) in the presence of inhibitors known to block CTL cytotoxic function. Bars represent the percentage of βL5 cell lysis by IGRP-CTLs **(J)** in the absence of inhibitors**, (K)** with anti-Fas antibody, (**L**) with Concanamycin; and (**M**) with Pan Caspase Inhibitor, Z-VAD-FMK. For representative histograms (**A**,

D, and **G**) all lines within a panel are from a single donor. Data plotted in **B**, **C**, **E**, **F** and **H-M** are mean ± SEM where T cells from each donor (7 donors for **B, C, E, F, and H-I** and 5 donors for **J-M**) were weighted equally. There were at least three separate experiments for each donor. Statistical significance was assessed by a non-parametric paired T-test with Wilcoxon Post Test Analysis. * P<0.05; ** P<0.01; ***P<0.001

Fig. 3: T1-IFN induces phosphorylation of STAT1 and STAT4 in IGRP-CTLs. (**A-C**) Western blot analysis of IGRP-CTLs treated with IFNα, IFNβ, or IFNγ for 15 minutes. (**A**) Representative blots and densitometry analysis of phosphorylated and total (**B**) STAT1 and (**C**) STAT4. (**D-F**) Time course analysis of pSTAT1 and pSTAT4 activation is shown by western blot. Densitometry was performed and are plotted against time for (**E**) STAT1 and (**F**) STAT4. Phospho flow cytometry was performed on IGRP-CTLs treated with IFNα (125U/mL & 1000U/mL) at several time points (5, 15, 30, 60, and 120min). (**G**) Representative histograms for phosphorylated STAT1 and STAT4 are displayed. (**H & I**) Mean fluorescence intensities (MFI) of pSTAT1 and pSTAT4 are plotted against time. (**J-L**) IGRP-CTL were primed with T1-IFN for 2 hours and assessed for T-bet and Eomes expression by flow cytometry. Representative histograms and MFI of (**J**) T-bet and (**K**) Eomes is displayed. **(L)** IGRP-CTL were pretreated with rapamycin for 16 hours, primed with IFNα for 2 hours, and subsequently assessed for granzyme B (GZMB) expression by flow cytometry (representative histograms and MFI are plotted). For representative western blots and histograms (**A**, **D**, **G, and J-L**) all lanes or lines within a panel are from a single donor. Data plotted in **B**, **C**, **E**, **F,** and **H-L** are mean ± SEM; T cells from each donor (at least 3 donors for **B, C, E, F, and L,** 5 donors for **H and I, and** 8 donors for **J and K**) were weighted equally. There were at least three separate experiments for each donor. Statistical significance was assessed by a non-parametric paired T-test with Wilcoxon Post Test Analysis. * P<0.05; ** P<0.01; ***P<0.001

Fig. 4: Inhibition of STAT4 reverses T1-IFN induced cytotoxicity. IGRP-CTLs were transfected with Accell siRNAs specific for STAT1, STAT4 or non-targeting controls for 72 hours. **(A-B)** RT-PCR analysis to assess gene silencing was performed for (**A**) STAT1 and (**B**) STAT4. All values were normalized relative to 18S mRNA expression. **(C-E)** IGRP-CTLs siRNA transfectants were primed with T1-IFN and assessed for granzyme B (GZMB) expression by flow cytometry. (**C**) Representative histograms, and (**D**) Mean Fluorescence Intensities (MFI) for GZMB are plotted. **(E)** Viability analysis on siRNA transfected CTLs is plotted**. (F-I)** IGRP-CTLs were pre-treated with Lisofylline (LSF) and analyzed for pSTAT4 activation by (**F**) western blot and (**G**) phospho flow cytometry. LSF treated CTLs were primed with IFNα and analyzed for GZMB expression by flow cytometry. (**H**) Representative histograms, and (**I**) MFI for GZMB are shown. For representative western blots and histograms (**C**, **F, and H**) all lanes or lines within a panel are from a single donor. Data plotted in **A**, **B**, **D**, **E**, **G**, and **I** are mean ± SEM; T cells from each donor (3 donors for **A** and **B,** at least 5 donors for **D**, **E,** and **G,** and at least 7 donors for **I**) were weighted equally. There were at least three separate experiments for each donor. Statistical significance was determined with a non-parametric paired T-test with Wilcoxon Post Test Analysis. * $P<0.05$; ** $P<0.01$; ***$P<0.001$

Fig. 5: T1-IFN induces pSTAT4 binding to the GZMB promoter to induce transcription**. (A-B)** qRT-PCR analysis of (**A**) *GZMB* and (**B**) *IFIH1* expression in IGRP-CTLs following 2-hour treatment with interferons. **(C-D)** Chromatin immunoprecipitation (CHIP)-qPCR with SYBR Green was performed to assess the binding of pSTAT1 and pSTAT4 to the GZMB promoter in IGRP-CTLs after treatment with IFNα for 1 hour. CHIP-qPCR representing the binding of STAT1 and STAT4 to the (**C**) putative proximal promoter- and (**D**) distal promoter-binding sites of GZMB is displayed. Data plotted in are mean ± SEM; T cells from 3 donors were weighted equally. There were at least three separate experiments for each donor. Statistical significance was determined by a non-parametric paired T-test with Wilcoxon Post Test Analysis. * $P<0.05$; ** $P<0.01$; ***$P<0.001$

Tables

Table 1. Peripheral blood donor sex (F, female; M, male) and age as well as $CD8^+$ T cell transduction efficiency for the experiments reported herein.

$CD8^+$ T Lymphocytes - Donor Information			
Sex	**Quantity**	**Mean Age (years) [Range]**	**Transduction Efficiency (%) [Range]**
F	7	27.64 [14.17-38.00]	75.47 [43.6- 93.3]
M	12	29.07 [12.50-46.67]	62.71 [37.5 - 84.2]

Figure 1

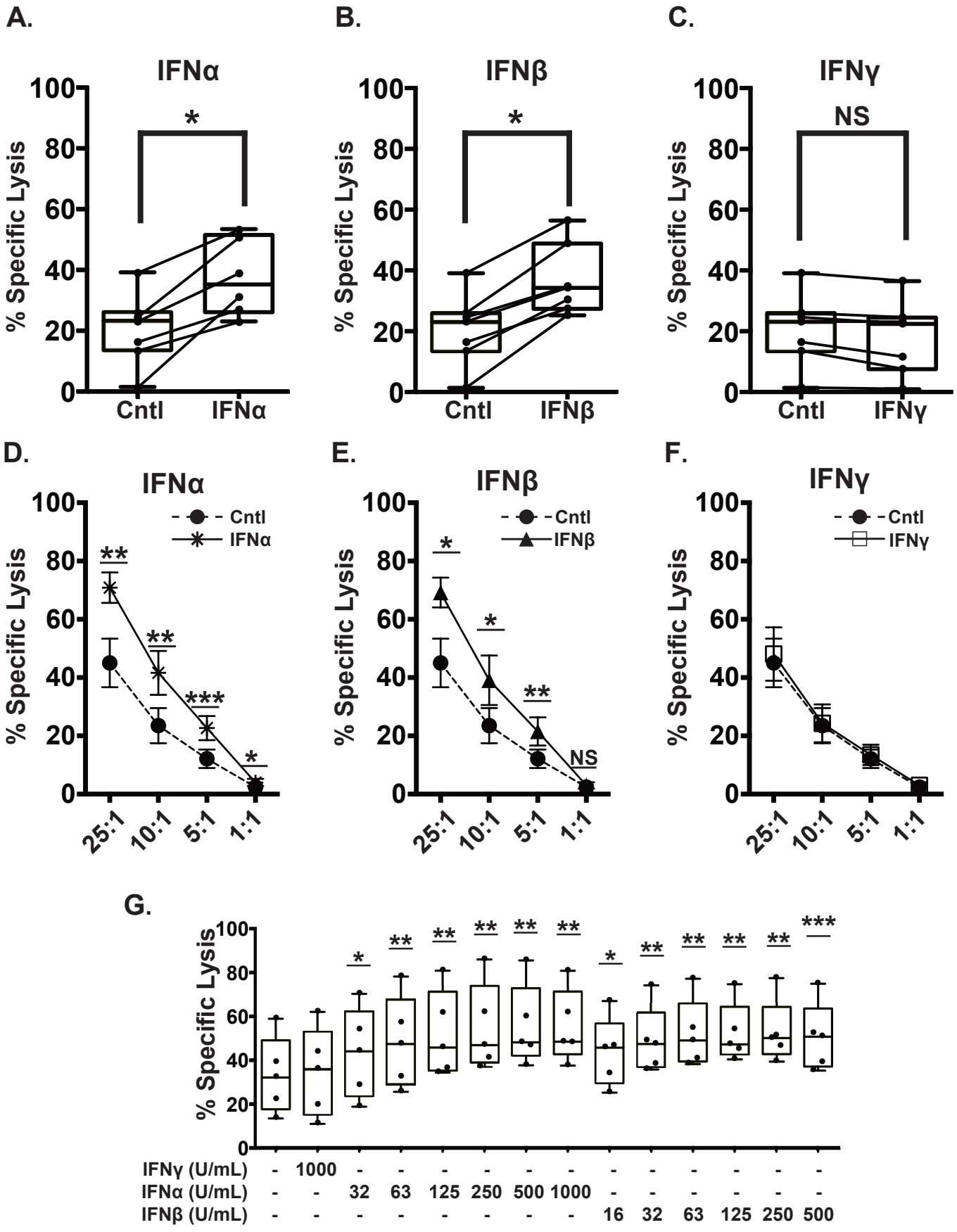
A.
IFNα
% Specific Lysis
Cntl
IFNα
*
B.
IFNβ
Cntl
IFNβ
*
C.
IFNγ
NS
Cntl
IFNγ
D.
IFNα
Cntl
IFNα
25:1
10:1
5:1
1:1
E.
IFNβ
Cntl
IFNβ
NS
F.
IFNγ
Cntl
IFNγ
G.
IFNγ (U/mL)
IFNα (U/mL)
IFNβ (U/mL)

Figure 2

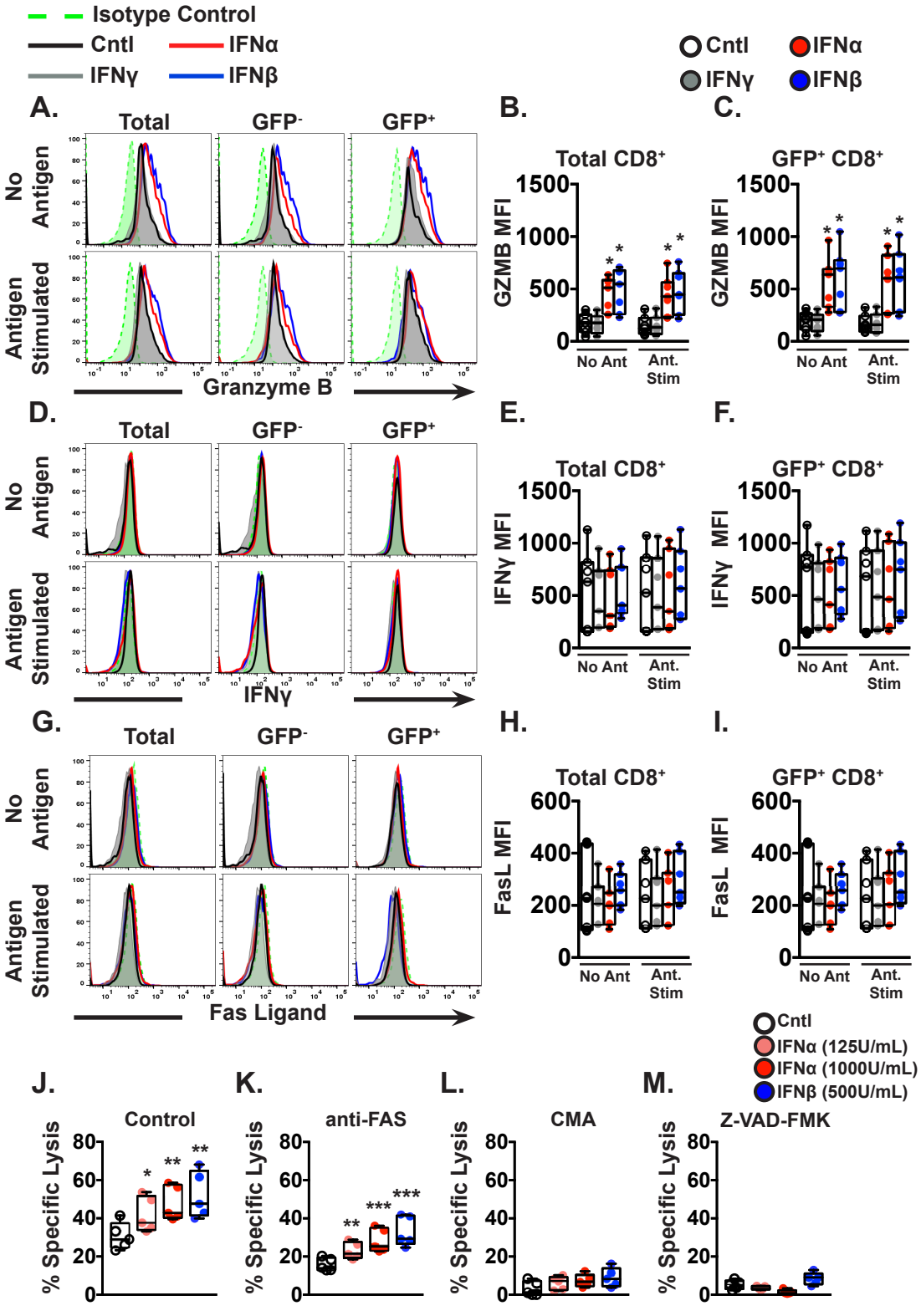
Isotype Control
Cntl
IFNα
IFNγ
IFNβ
A.
Total
GFP-
GFP+
No Antigen
Antigen Stimulated
Granzyme B
B.
Total CD8+
GZMB MFI
C.
GFP+ CD8+
No Ant
Ant. Stim
D.
IFNγ
E.
IFNγ MFI
F.
G.
Fas Ligand
H.
FasL MFI
I.
IFNα (125U/mL)
IFNα (1000U/mL)
IFNβ (500U/mL)
J.
Control
% Specific Lysis
K.
anti-FAS
L.
CMA
M.
Z-VAD-FMK

Figure 3

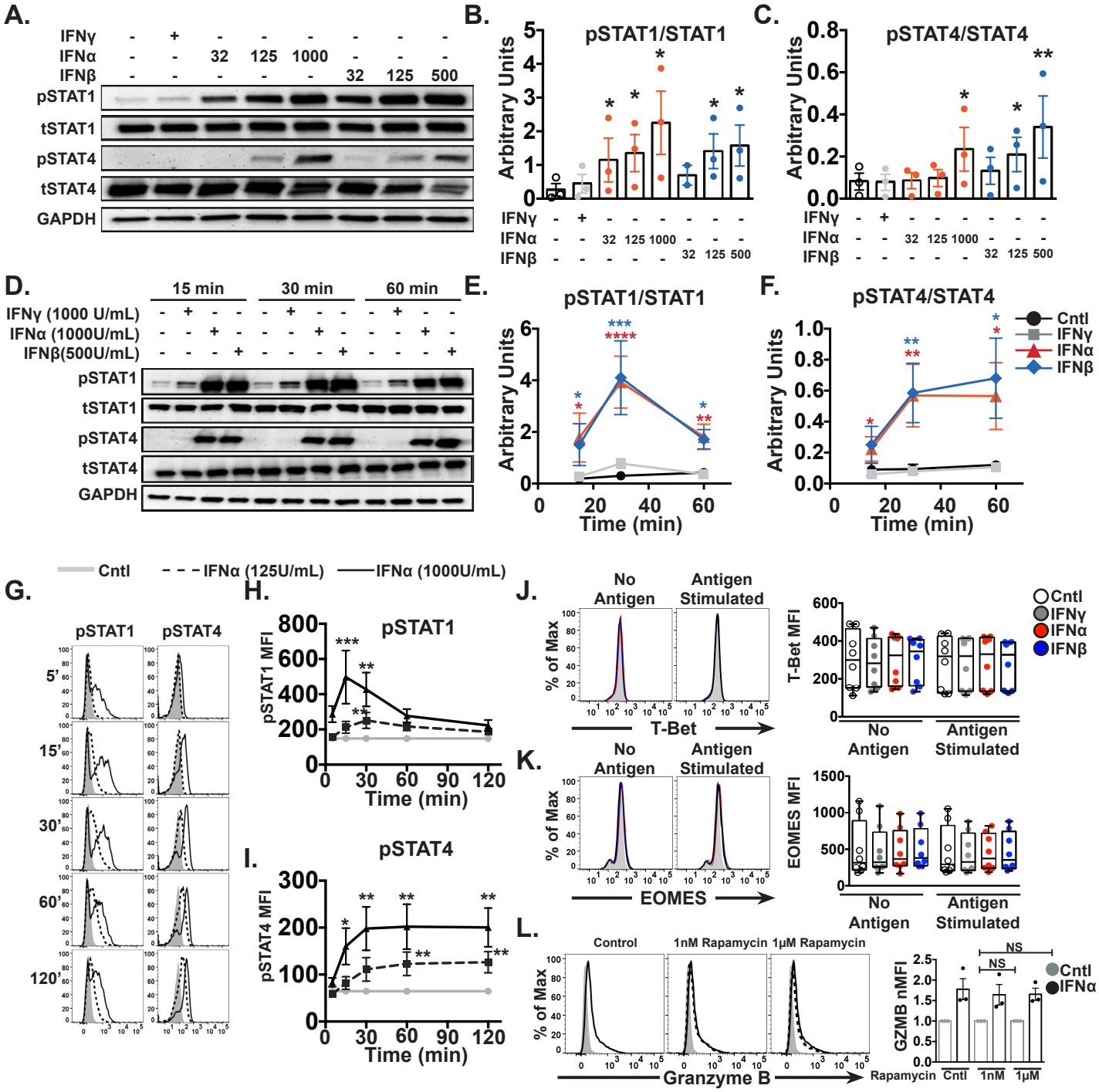
A.
IFNγ - + - - - - - -
IFNα - - 32 125 1000 - - -
IFNβ - - - - - 32 125 500
pSTAT1
tSTAT1
pSTAT4
tSTAT4
GAPDH
B.
pSTAT1/STAT1
Arbitrary Units
C.
pSTAT4/STAT4
Arbitrary Units
D.
15 min
30 min
60 min
IFNγ (1000 U/mL)
IFNα (1000U/mL)
IFNβ(500U/mL)
pSTAT1
tSTAT1
pSTAT4
tSTAT4
GAPDH
E.
pSTAT1/STAT1
Arbitrary Units
Time (min)
F.
pSTAT4/STAT4
Arbitrary Units
Time (min)
Cntl
IFNγ
IFNα
IFNβ
Cntl
IFNα (125U/mL)
IFNα (1000U/mL)
G.
pSTAT1
pSTAT4
5'
15'
30'
60'
120'
H.
pSTAT1
pSTAT1 MFI
Time (min)
I.
pSTAT4
pSTAT4 MFI
Time (min)
J.
No Antigen
Antigen Stimulated
% of Max
T-Bet
T-Bet MFI
K.
EOMES
EOMES MFI
L.
Control
1nM Rapamycin
1μM Rapamycin
Granzyme B
GZMB nMFI
Rapamycin
Cntl
1nM
1μM
NS

Figure 4

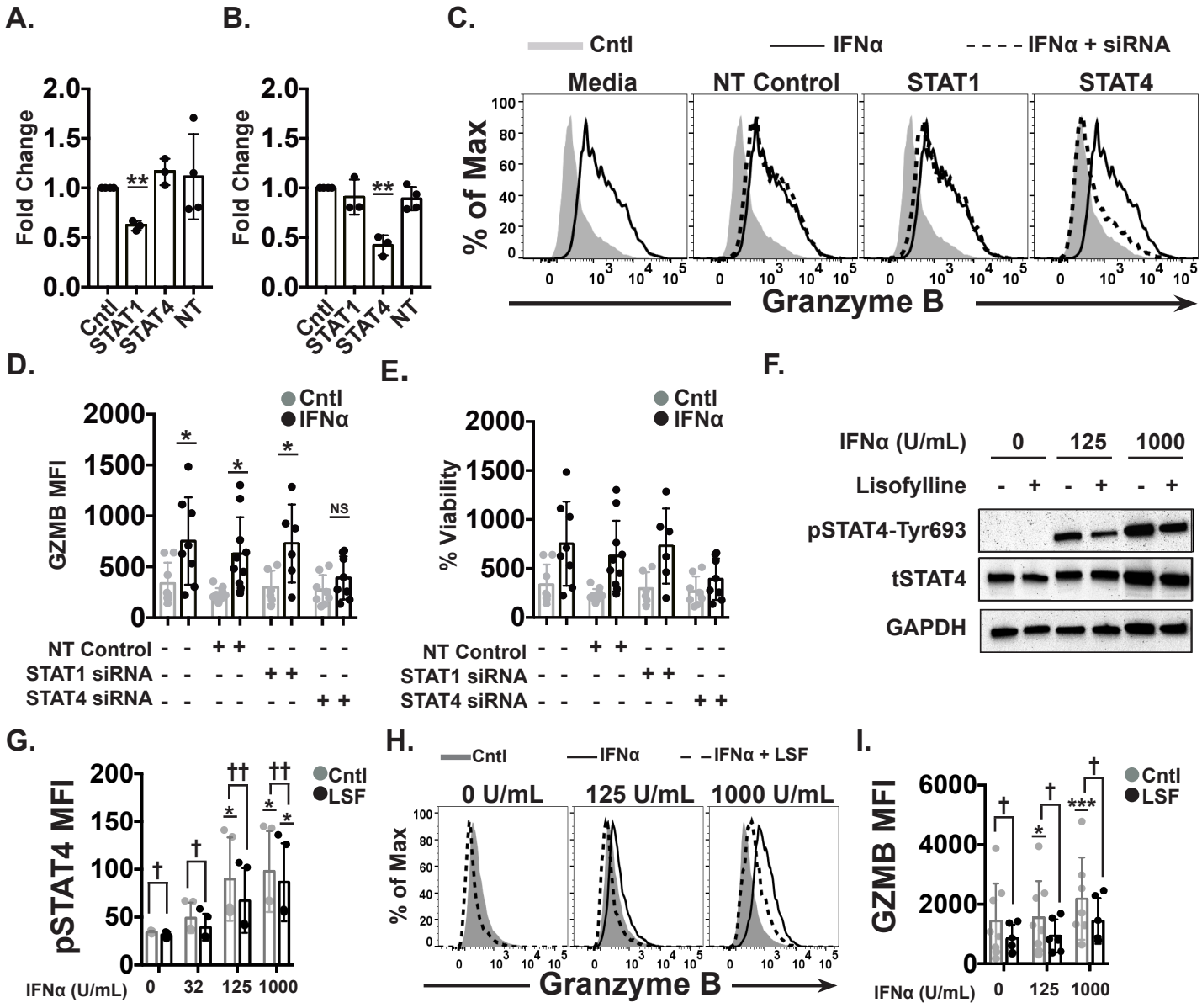
A.
B.
C.
Fold Change
Cntl
STAT1
STAT4
NT
Cntl
IFNα
IFNα + siRNA
Media
NT Control
STAT1
STAT4
% of Max
Granzyme B
D.
E.
F.
GZMB MFI
% Viability
NT Control
STAT1 siRNA
STAT4 siRNA
NS
IFNα (U/mL)
Lisofylline
pSTAT4-Tyr693
tSTAT4
GAPDH
G.
H.
I.
pSTAT4 MFI
LSF
0 U/mL
125 U/mL
1000 U/mL
GZMB MFI

Figure 5

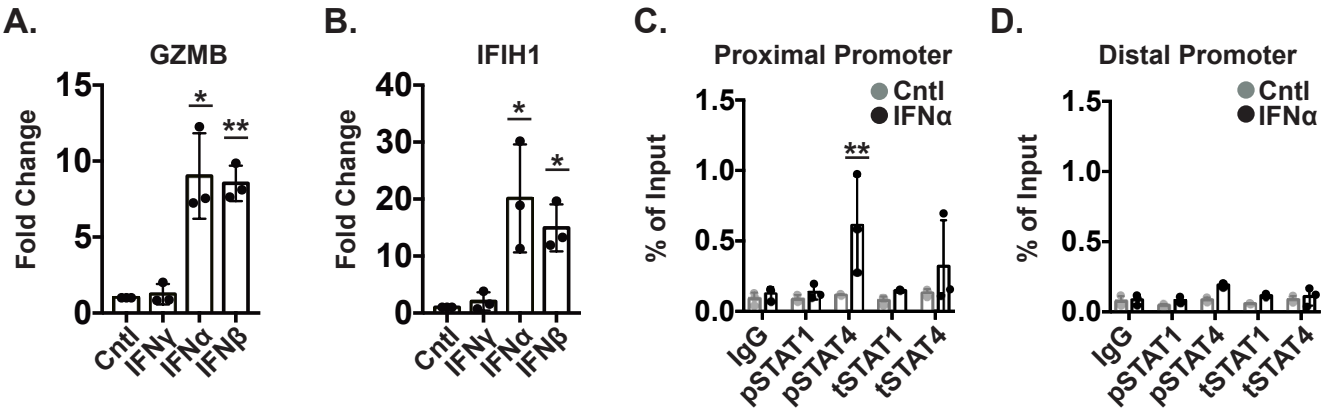
A.
GZMB
Fold Change
15
10
5
0
*
**
Cntl
IFNγ
IFNα
IFNβ
B.
IFIH1
Fold Change
40
30
20
10
0
*
*
Cntl
IFNγ
IFNα
IFNβ
C.
Proximal Promoter
Cntl
IFNα
% of Input
1.5
1.0
0.5
0.0
**
IgG
pSTAT1
pSTAT4
tSTAT1
tSTAT4
D.
Distal Promoter
Cntl
IFNα
% of Input
1.5
1.0
0.5
0.0
IgG
pSTAT1
pSTAT4
tSTAT1
tSTAT4

Supplemental Table 1

Antibody Information

Antibody	Clone	Manufacturer
Anti-CD8	SK1	BioLegend
Anti-CD45RA	HI100	BioLegend
Anti-CD45RO	UCHL1	BioLegend
Anti-Granzyme B	GB11	BioLegend
Anti-Fas Ligand	NOK-1	BioLegend
Anti-IFNγ	4S.B3	BioLegend
Anti-T-bet	4B10	BioLegend
Anti-Eomes	WD1928	eBiosciences
Anti-phospho-STAT1	KIKSI0803	eBiosciences
Anti-phospho-STAT4	4LURPIE	eBiosciences
Anti-STAT1	9172	Cell Signaling Technologies
Anti-phospho-STAT1	9167	Cell Signaling Technologies
Anti-STAT4	C46B10	Cell Signaling Technologies
Anti-phospho-STAT4	D2E4	Cell Signaling Technologies
Anti-Histone H3	D2B12	Cell Signaling Technologies
Anti-Rabbit IgG	2729	Cell Signaling Technologies
Anti-Rabbit IgG, HRP	7074	Cell Signaling Technologies
Anti-GAPDH	G-9 (sc-365062)	Santa Cruz
Anti-Mouse IgG	sc-2302	Santa Cruz

Supplemental Table 2

Taq Man Probes

Probe	Probe ID
STAT1	Hs01013996_m1
STAT4	Hs01028017_m1
Granzyme B	Hs00188051_m1
GAPDH	Hs02758991_g1
18S	Hs03003631_g1

Supplemental Table 3

CHIP Primer Sequences

Antibody	Clone
GZMB Promoter Primer Pair 1 Forward	5’-tcacttcataggcttgggttcct -3’
GZMB Promoter Primer Pair 1 Reverse	5’- ctctgggtgcttgtgtgagaatc -3’
GZMB Promoter Primer Pair 2 Forward	5’-ctgtgagcctgttatgtgctgag -3’
GZMB Promoter Primer Pair 2 Reverse	5’- ggacgtttgtggtgctaaattgc -3’

Supplemental Table 4. IFNα and IFNβ pretreatment of human IGRP-CTL for 2 hours increases the lytic function of these cells. These data accompany Figures 1D-1F. Data reported in this table are the averages of the technical replicates for the individual donor. These averages were used to generate the Mean ± SEM reported in Figures 1D-1F.

E:T Ratio = 25:1

Treatment	Donor 1	Donor 2	Donor 3	Donor 4	Donor 5	Donor 6
Control	44.50	24.80	68.40	64.60	18.10	49.78
IFNα	76.30	63.50	88.40	74.20	50.50	72.21
IFNβ	60.35	69.70	88.80	74.40	52.00	69.89
IFNγ	50.30	24.20	65.20	75.30	18.77	54.76

E:T Ratio = 10:1

Treatment	Donor 1	Donor 2	Donor 3	Donor 4	Donor 5	Donor 6
Control	19.30	12.02	33.80	47.20	7.20	21.58
IFNα	37.90	34.30	62.50	65.80	20.30	28.88
IFNβ	26.37	30.30	66.20	65.10	21.30	25.21
IFNγ	22.40	11.12	31.50	51.70	7.40	21.66

E:T Ratio = 5:1

Treatment	Donor 1	Donor 2	Donor 3	Donor 4	Donor 5	Donor 6
Control	9.20	7.70	19.11	24.00	3.80	9.02
IFNα	20.50	15.60	35.60	35.00	12.00	17.43
IFNβ	13.71	15.90	36.70	36.00	9.30	17.60
IFNγ	11.80	6.80	18.70	28.10	5.20	10.14

E:T Ratio = 1:1

Treatment	Donor 1	Donor 2	Donor 3	Donor 4	Donor 5	Donor 6
Control	2.70	2.80	6.10	1.05	0.63	1.38
IFNα	4.30	5.20	9.40	1.80	1.25	1.95
IFNβ	1.98	4.80	7.70	1.60	0.82	1.12
IFNγ	4.10	2.30	4.20	6.80	0.01	0.79

Supplemental Figure 1

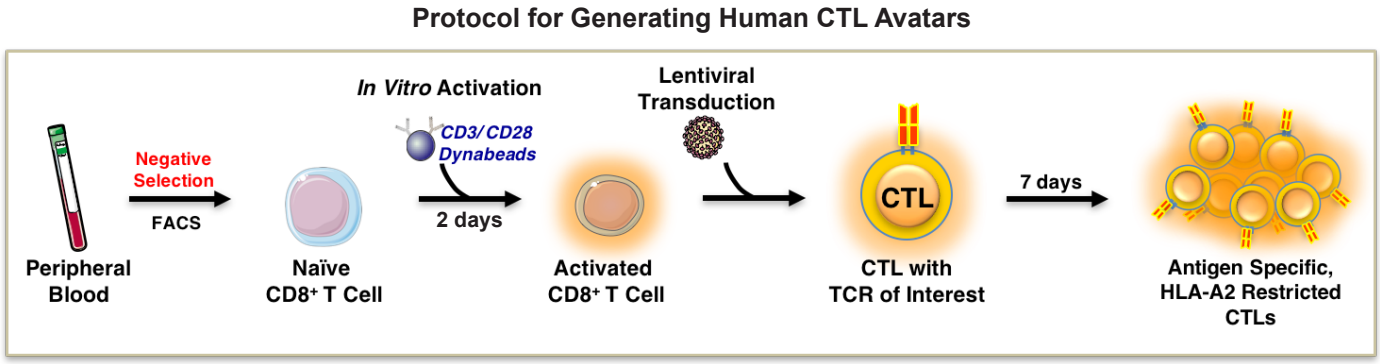

Supplemental Figure 1. Schematic representation of protocol for generating human CTL avatars. Peripheral blood samples are obtained from consenting human subjects. Samples undergo negative selection and FACs cell sorting for isolation of naïve CD8+ T lymphocytes. These cells are subsequently activated in vitro using CD3/CD28 conjugated beads, which act to mimic TCR and co- stimulatory signals that trigger T cell proliferation and differentiation. After 48 hours, T cells are transduced with lentiviral vectors which permanently integrate sequences for antigen specific TCRs into the genome of the lymphocyte. Newly transduced avatars are expanded over an additional 7 days to yield a large pool of antigen-specific CTLs for study.

Supplemental Figure 2

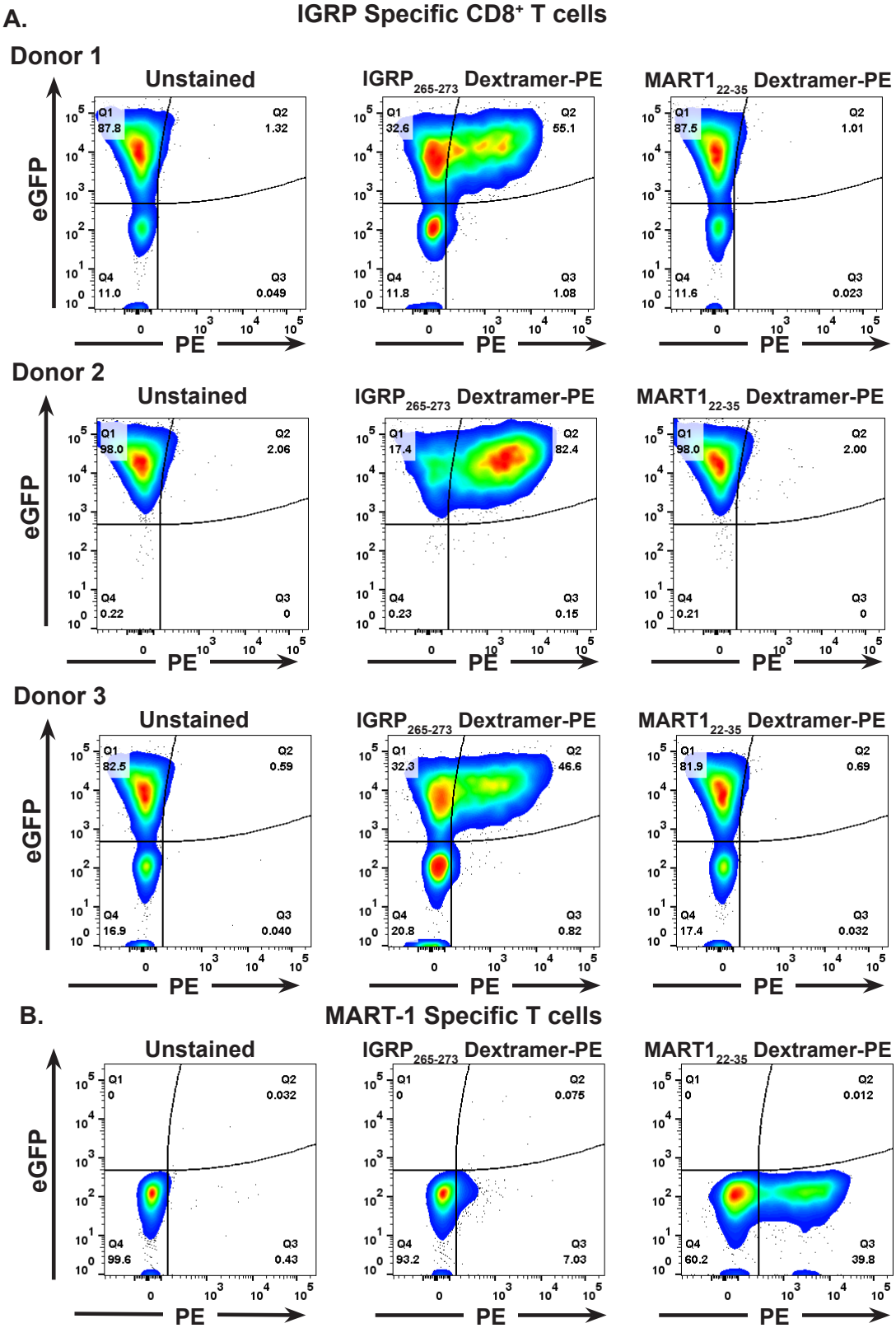

Supplemental Figure 2. Human CTL Avatars are Antigen Specific. Following expansion, human CTL avatars were stained with PE-conjugated dextramers and subjected to flow cytometric analysis. (A) Dot plots of IGRP-specific CTL avatars from three donors are displayed. Dextramer binding as displayed by PE fluorescence is compared to eGFP expression, which serves as a fluorescent tag for positively transduced IGRP CTLs. IGRP-specific CTLs selectively bind to the $IGRP_{265-273}$ dextramer, but show no binding to the $MART\text{-}1_{22-35}$ dextramer. (B) Additonally, MART-1-specific CTL avatars were generated,stained, and analyzed for dextramer binding by flow cytometry. While the lentiviral construct used to generate these human CTL avatars does not contain a fluorescent tag, these cells selectively bind the $MART\text{-}1_{22-35}$ dextramer serving as a positive control for the $MART\text{-}1_{22-35}$ dextramer.

Supplemental Figure 3

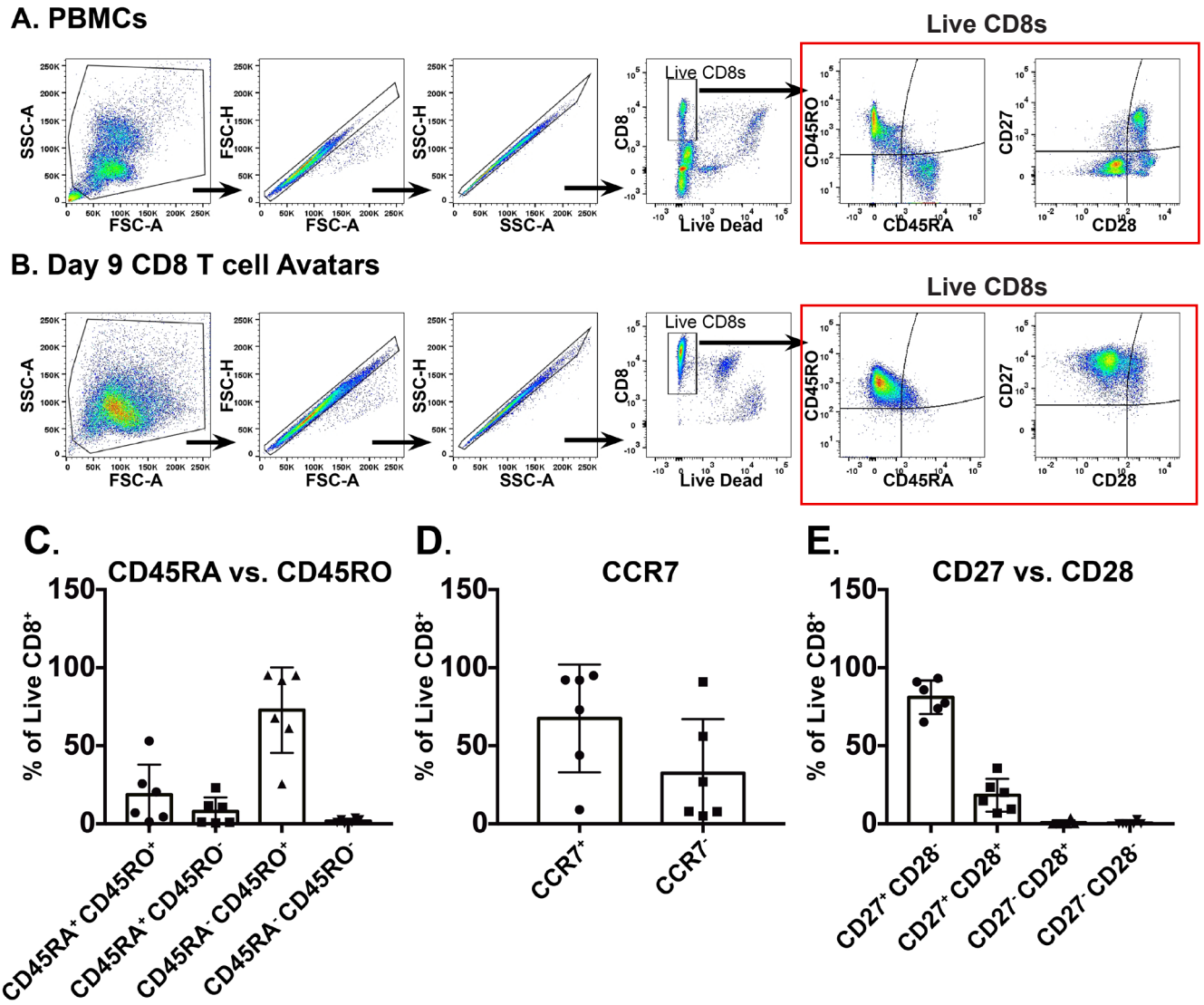

Supplemental Figure 3. CTL avatars display primarily an effector/ effector memory phenotype with marked levels of CD27 expression. (A & B). The gating strategy for the surface characterization of PBMCs, which were used as a gating control, as well as the CTL avatars. (C) Compares the percentage of live CD8+ T cells that show differential profiles for CD45RA and CD45RO expression. (D) Displays the percentage of live CD8+ T cells that are positive or negative for CCR7. (E) Compares the percentage of live CD8+ T cells that show differential profiles for CD27 and CD28 expression.

Supplemental Figure 4

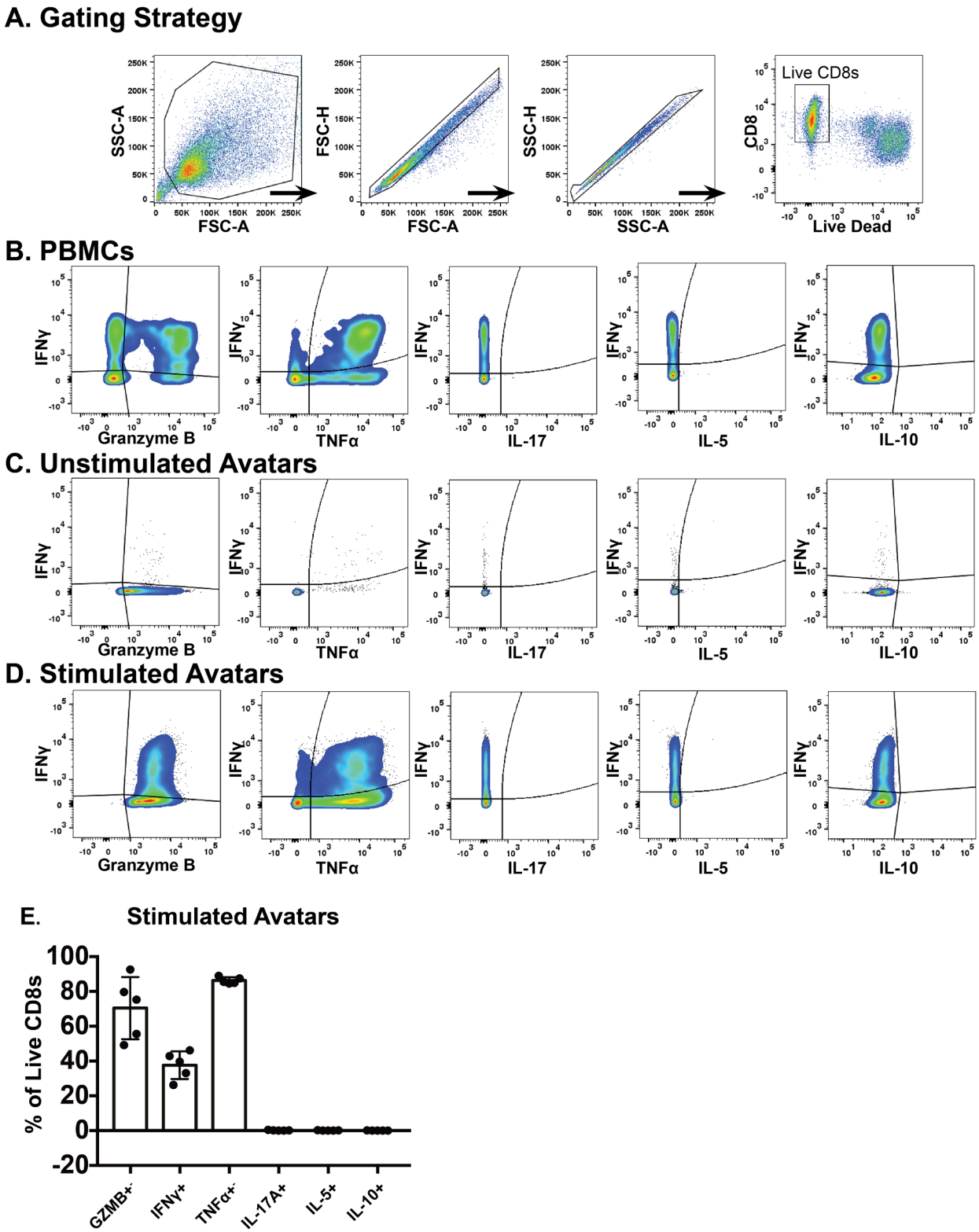

Supplemental Figure 3. CTL Avatars are characterized by high levels of granzyme B and robust production of IFNγ and TNFα following PMA/Ionomycin stimulation. A). The gating strategy used for gating of live CD8+ T cells. B-D) Compares the cytotoxin and cytokine profiles for control PBMCs, unstimulated CTL avatars, and CTL avatars stimulated with PMA and Ionomycin. E) Compares the percentage of live stimulated CTL avatars that are positive for Granzyme B (GZMB), IFNγ, TNFα, IL-17A, IL-5, and IL10.

Supplemental Figure 5

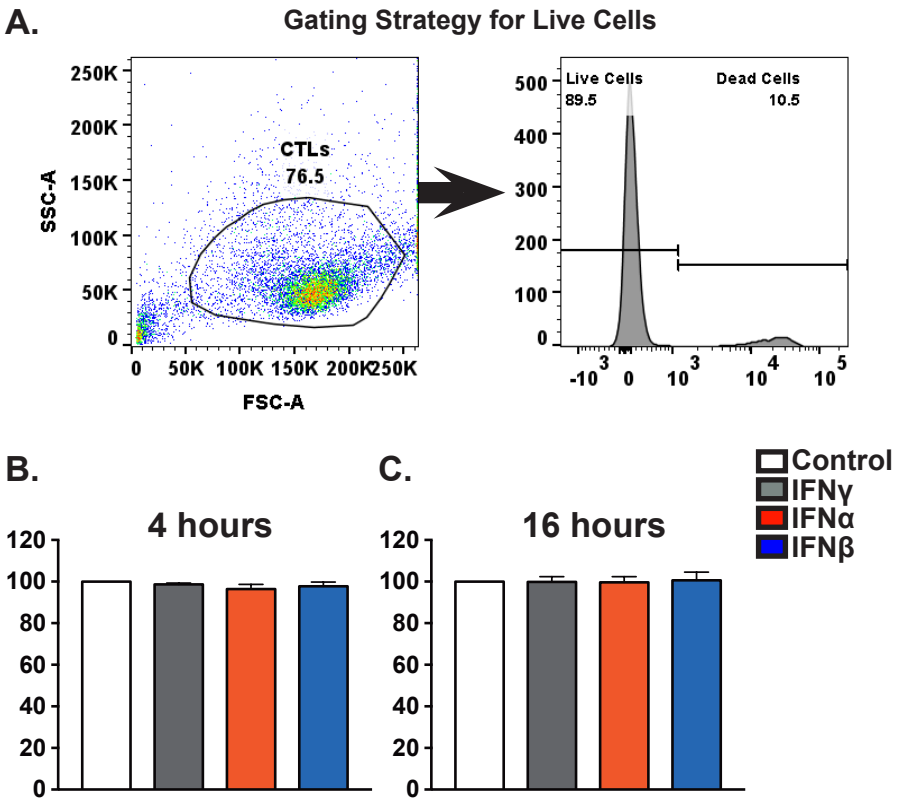

Supplemental Figure 5. Viability Analysis of IGRP CTLs following IFN-priming
Viability analysis was performed on IGRP-CTLs using flow cytometry following 2-hour cytokine priming. Representative Gating Strategy shown (A). Viability determined by Live/Dead Viability dye staining after 2 hour IFN-priming and 4 hour incubation (B) or 16 hour incubation (C) in media.

Supplemental Figure 6

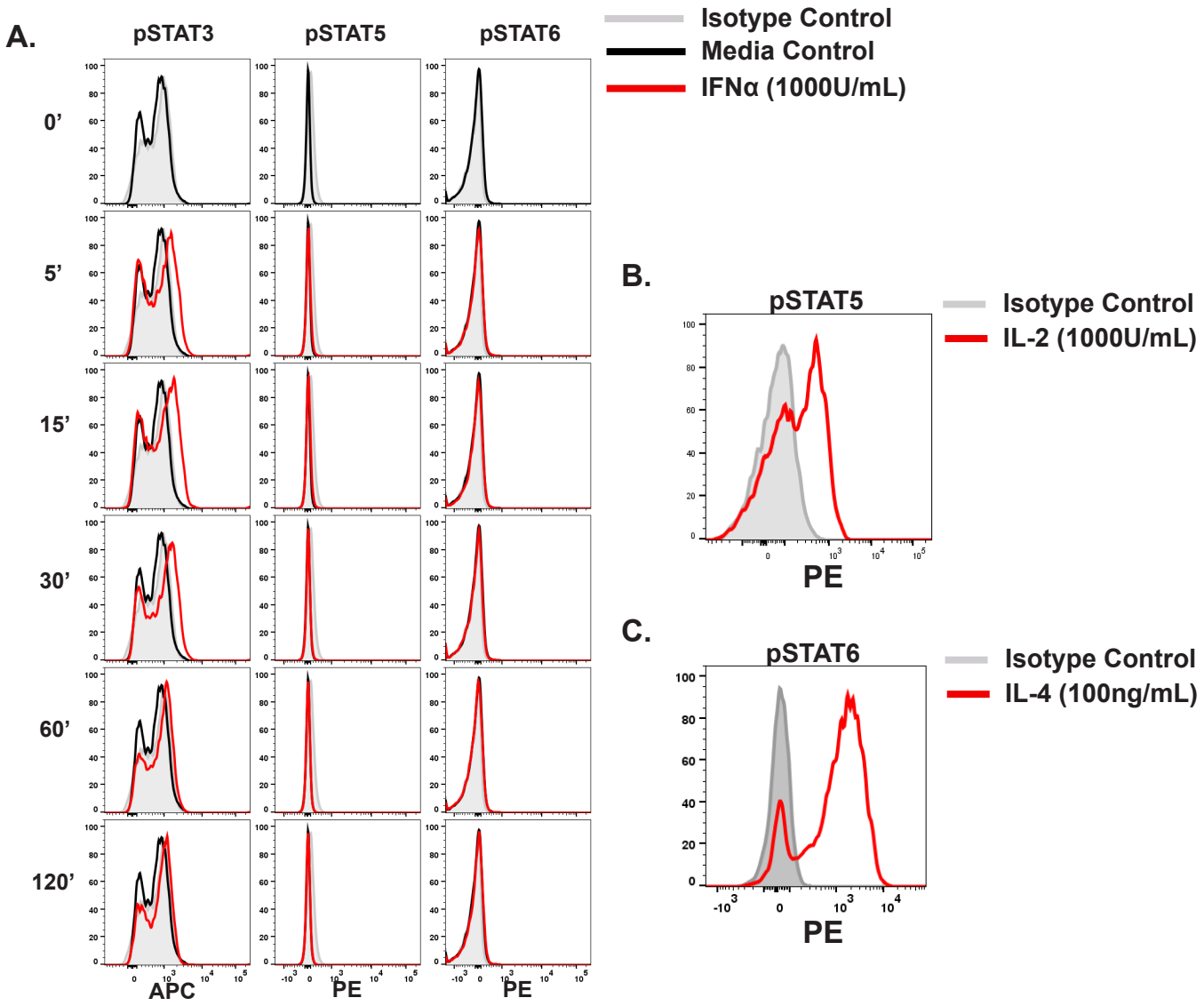

Supplemental Figure 6. Phospho Flow Cytometry for pSTAT3, pSTAT5, and pSTAT6 following T1-IFN Treatment. (A) Phospho Flow Cytometry was performed on IGRP-CTLs treated with IFNα (1000U/mL) over several time points (5, 15, 30, 60, and 120min) to characterize T1-IFN STAT signaling. Representative histograms for phosphorylated STAT3, STAT5, and STAT6 are displayed. (B) IGRP-CTLs were treated with IL-2 (1000U/mL) for 30 minutes and assessed for phosphorylated STAT5 by phospho flow cytometry. A representative histogram is displayed. (C) IGRP-CTLs were treated with IL-4 (1000U/mL) for 30 minutes and assessed for phosphorylated STAT6 by phospho flow cytometry. A representative histogram is displayed.

Supplemental Figure 7

Legend

Proximal STAT1/STAT4 Binding Site

STAT 1 Binding Site

Distal STAT1/STAT4 Binding Site

A.

GZMB Promoter Primer Pair 1

Product Size: 111

Forward Primer: 5'-tcacttcataggcttgggttcct -3'

Reverse Primer: 5'- ctctgggtgcttgtgtgagaatc -3

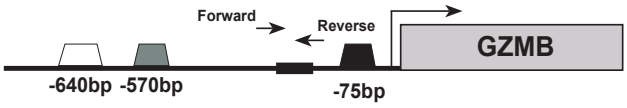

B.

GZMB Promoter Primer Pair 2

Product Size: 152

Forward Primer: 5'-ctgtgagcctgttatgtgctgag -3'

Reverse Primer: 5'- ggacgtttgtggtgctaaattgc -3'

Supplemental Figure 7. Information regarding Primer Pairs used for Chromatin Immunoprecipitation
Schematics detailing the sequences, expected size product and position of the primer pairs within the promoter of granzyme B are displayed (A & B).